REDUCED STATE BCJR ALGORITHMS FOR ONE- AND TWO-DIMENSIONAL EQUALIZATION

Ying Zhu, Benjamin Belzer and Krishnamoorthy Sivakumar

School of EECS, Washington State University, Pullman WA 99164-2752
yzhu2@eecs.wsu.edu, belzer@eecs.wsu.edu, siva@eecs.wsu.edu

ABSTRACT

We consider BCJR-like soft-input soft-output (SISO) iterative detection algorithms for 1D and 2D binary-input ISI channels with AWGN. The complexity of BCJR algorithms grows exponentially with the size of the ISI mask and is an important concern with their implementation. We consider new techniques to reduce the complexity of BCJR algorithms by decreasing the effective number of states in the trellis. The proposed state reduction technique does particularly well for mixed phase sequence ISI masks, which have higher weights for the center taps and lower weights for the peripheral taps. Other complexity reduction techniques proposed in the literature perform poorly for such masks. Moreover, the complexity of the proposed state reduction technique is comparable to other reduced complexity techniques reported in the literature. Experimental results are provided to demonstrate the advantages of the proposed state reduction technique.

Index Terms— Intersymbol interference, Equalization, BCJR algorithm, Reduced complexity

1. INTRODUCTION

BCJR-based SISO iterative algorithms (based on [1]) have been successfully employed for both 1D [2] and 2D [3–6] equalization of finite-state ISI channels with AWGN. Unlike hard decision algorithms (such as the standard Viterbi algorithm), SISO algorithms provide soft information, which can be iteratively refined to ultimately provide a better hard decision. The computational complexity of these algorithms grows exponentially with the size of the channel impulse response, or "mask". To reduce complexity, a number of reduced-state BCJR algorithms have been proposed, including, e.g., the reduced state BCJR (RS-BCJR) of [7], the (quite similar) RS-SISO algorithm of [8], the minimum sequence metric reduced-state SISO (MSM RS-SISO) of [8], and the M-BCJR algorithm of [9]. These algorithms, when used for equalization of finite-length 1D ISI channels, typically perform reasonably close to their corresponding full-state versions when the channels are minimum- or maximum-phase. However, their performance suffers with mixed-phase channels that have relatively high-magnitude center taps and lower magnitude peripheral taps; we refer to such channel masks as "center-weighted."

The contributions and organization of the present paper are as follows. In section 2, we present a new 1D truncated state SISO algorithm. The new algorithm, based on the MSM RS-SISO of [8], uses a truncation scheme more appropriate for center-weighted masks. Simulation results in subsection 2.1 show that the new 1D algorithm significantly outperforms MSM RS-SISO for center weighted masks. In section 3, we extend the new algorithm to work with the iterative row-column soft decision feedback algorithm (IRCSDFA) (of [3]) for 2D-ISI channels. The IRCSDFA is one of the best performing 2D-ISI equalizers in the literature, and attains performance close to the maximum-likelihood (ML) bound for a number of 2D ISI channels. Simulation results presented in subsection 3.1 show that the new 2D reduced-state IRCSDFA outperforms versions employing the MSM RS-SISO and M-BCJR reduced state algorithms, for center-weighted 2D-ISI masks. In section 4, we draw conclusions and point out several areas where additional work is needed.

1.1. Channel Model, Notation, and Related Work

We consider the finite-length ISI channel

$$\mathbf{r} = \mathbf{h} * \mathbf{a} + \mathbf{w}, \tag{1}$$

where $\mathbf{h}$ is the channel mask, $\mathbf{a}$ is the data, $\mathbf{w}$ contains independent and identically distributed (i.i.d.) Gaussian random variables of 0 mean and variance $N_0/2$, and "*" indicates 1- or 2-dimensional convolution. For the 1D case, $\mathbf{h} = \{h_i\}$, $0 \leq i \leq L-1$, and $\mathbf{a} = \{a_k\} \in \{-1, 1\}$, $0 \leq k \leq N-1$. For 2D, $\mathbf{h} = \{h_{i,j}\}$, $0 \leq i,j \leq L-1$, and $\mathbf{a} = \{a_{k,l}\}$, $0 \leq k,l \leq N-1$. At the kth input symbol, the input to the 1D ISI channel is a_k, and the state is the previous $L-1$ symbols $a_{k-1}, \ldots, a_{k-L-1}$. This leads to a trellis diagram with 2^{L-1} states and two branches leaving (and entering) each state.

At each trellis stage in its forward pass, the M-BCJR algorithm of [9] selects the M states with the highest forward state probabilities $\alpha(m)$ and retains only those states and their connecting branches. The backward pass employs the same strategy, using the backward state probabilities $\beta(m)$ to independently choose the backward-pass active states. In this paper, we employ a simplified M-BCJR that runs the backward pass on the states and branches selected during the forward pass. The standard log-MAP version of BCJR is then employed to estimate the *a posteriori* probabilities (APPs) of the input symbols.

The MSM RS-SISO of [8] defines truncated forward and backward state vectors as in Fig. 1, which shows a simple example for $L = 3$. The full-state trellis would have four states, but the truncated-state trellis has only two states. A min-log version of the BCJR algorithm is employed, with different branch metrics $\lambda_k^f(i,j)$ and $\lambda_k^b(i,j)$ for the forward and backward passes; here i and j are state indices of the reduced-state trellis. The branch metrics correspond to the negative log of the $\gamma_k(i,j)$ state transition probabilities. The branch outputs necessary to compute the $\gamma_k(i,j)$s depend on the missing symbols $k-2$ and $k+2$ for the forward and backward

The authors would like to thank the National Science Foundation for providing support for the work presented in this paper, under grant CCF-0635390.

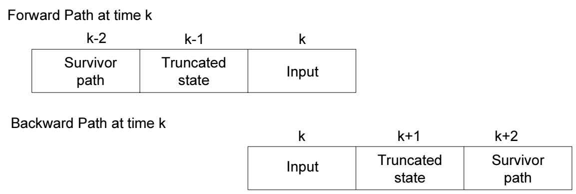

Fig. 1. Truncated state diagram for the MSM RS-SISO of [8], for a 1D mask of length $L = 3$.

passes; these missing symbols are estimated by keeping track of surviving paths (in both the forward and backward directions) into the truncated states. The log-min formulation means that the update equations in both directions are similar to those of the Viterbi algorithm. The update equations from [8] are now briefly summarized, as they are the same equations used in the new algorithm presented in section 2. The forward and backward state metric updates are

$$\delta_{k+1}(j) = \min_{i \in \mathcal{F}(j)} [\delta_k(i) + \lambda_{k+1}^f(i,j)] \tag{2}$$

$$\eta_k(i) = \min_{j \in \mathcal{B}(i)} [\eta_{k+1}(j) + \lambda_{k+1}^b(i,j)], \tag{3}$$

where $\mathcal{F}(j) = \{i : i \rightarrow j \text{ is an allowed forward transition}\}$ and $\mathcal{B}(i) = \{j : i \leftarrow j \text{ is an allowed backward transition}\}$. The soft output metrics for symbol a_k are computed by minimizing over the sums of the relevant forward and backward state metrics:

$$M^o(a_k = m) = \min_{j \in \mathcal{C}(m)} [\delta_k(j) + \eta_k(j)], \tag{4}$$

where $\mathcal{C}(m) = \{j : \text{at time } k+1\text{, state element } a_k = m\}$, and $m \in \{-1, 1\}$. Extrinsic information can be passed either to subsequent iterations of the 1D MSM RS-SISO ("self-iterations"), or to a MSM RS-SISO running in another scanning direction (for 2D ISI detection); the output extrinsic information metric is

$$M_e^o(a_k = m) = M^o(a_k = m) - M^i(a_k = m), \tag{5}$$

where $M^i(a_k = m)$ denotes input extrinsic information.

2. 1D REDUCED STATE ALGORITHMS FOR CENTER-WEIGHTED MASKS

For center weighted masks with small magnitude peripheral taps, the distance differences between surviving path candidates are very small, causing the MSM RS-SISO of [8] to choose incorrect surviving paths and leading to poor detection performance. To solve this problem, we redefine the forward and backward truncated state vectors as in Fig. 2, which shows an example for $L = 3$. In these diagrams, the leading bits in the forward and backward directions, which are the input bits in the full-state version, are simply ignored; their contribution to the branch outputs is small due to the small peripheral taps and can therefore be neglected. The indexing of the update equations (2)-(4) is adjusted to account for the offset between the estimated input bit in the forward and backward directions in the new state vectors; no such offset is present in the original state vector definitions shown in Fig. 1. Because the truncated bits are ignored, there is no need to estimate them using surviving paths.

For the 1D mask of length $L = 3$, the fully connected trellis has four states with two branches out of each state. By comparison, both the algorithm of [8] (due to Chen and Chugg) and our proposed algorithm has two states with two branches out of each state, which is equivalent in complexity to the M-BCJR algorithm with $M = 2$.

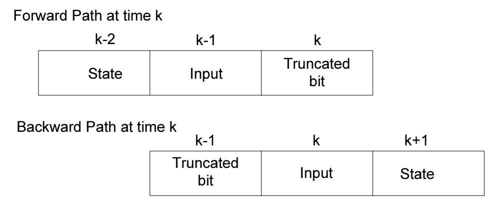

Fig. 2. Truncated state diagram for the new MSM RS-SISO algorithm for center-weighted masks of length $L = 3$.

2.1. Simulation Results

We consider the 1D channel $[\alpha \; 1 \; \alpha]$ with $\alpha = 0.1, 0.2, 0.8$ and 1.0. We compare the performance of our proposed algorithm with that of the M-BCJR algorithm [9] for $M = 2$ and Chugg's algorithm [8]. The union upper bound on the performance of the ML equalizer is also shown for comparison; this bound is tight at high SNR. The results for $\alpha = 0.1, 0.2$ are shown in Fig. 3; this figure also shows the results of simple hard decision demodulation (without equalization) for these channels. Fig. 4 depicts similar results for $\alpha = 0.8, 1.0$. With reference to the channel model (1), the SNR in all simulations reported in this paper is

$$\text{SNR} = 10 \log_{10} \left(\text{var}\left[\mathbf{a} * \mathbf{h}\right] / \sigma_w^2 \right), \tag{6}$$

where $*$ denotes 1- or 2-D convolution, and σ_w^2 is the variance of the elements of the noise vector $\mathbf{w}$ in (1).

When $\alpha = 0.1$ or 0.2, M-BCJR with $M = 2$ gives the best performance, which is very close to the ML bound. For $\alpha = 0.1$, our proposed algorithm is about 0.7 dB away and Chugg's algorithm is about 17 dB away from the ML bound, while the hard-decision curve is about 2.9 dB from the bound. For $\alpha = 0.2$, our proposed algorithm is about 3 dB away and Chugg's algorithm is about 11 dB away from the ML bound, while the hard-decision curve is about 12.5 dB from the bound. When $\alpha = 0.8$ or 1.0, M-BCJR with $M = 2$ again gives the best performance, which is 0.6 dB away from the ML bound. For $\alpha = 0.8$ ($\alpha = 1.0$), Chugg's algorithm is 0.8 dB (0.9 dB) away from the ML bound, whereas our proposed algorithm completely fails in both cases. All comparisons are done at a BER of 10^{-4}.

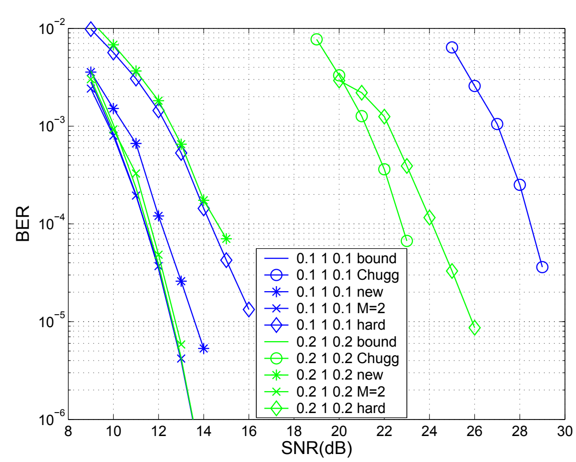

Fig. 3. 1D simulation results for masks $[0.1 \; 1 \; 0.1]$ and $[0.2 \; 1 \; 0.2]$.

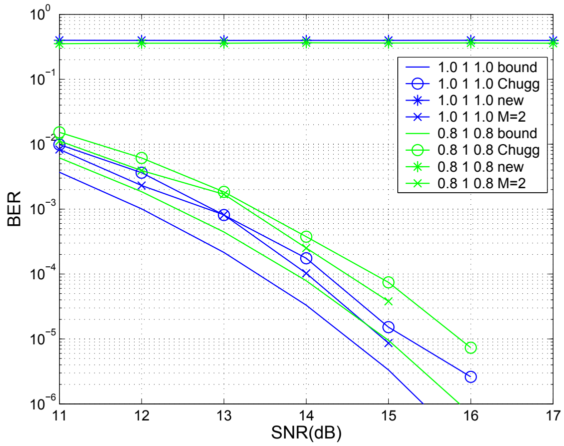

Fig. 4. 1D simulation results for masks [0.8 1 0.8] and [1 1 1].

Since our proposed algorithm truncates one state bit, it is expected to perform well when the contribution of the truncated mask element is small. In the current example, this happens when the value of α is small.

3. 2D REDUCED STATE ALGORITHMS FOR CENTER-WEIGHTED MASKS

Fig. 5 shows the truncated state and input block for the row-trellis of the iterative row-column soft decision feedback algorithm (IRCSDFA) of [3], for a 3×3 ISI mask. This modified IRCSDFA uses MSM RS-SISOs (like those in [8]) in row and column directions; the SISOs iteratively exchange extrinsic information until convergence occurs. A similar input block, rotated right by 90 degrees, defines the column trellis.

Trellis generation for the 3×3 mask on the mth image row is initiated by placing the input marked (m, n) in Fig. 5 (the uppermost of the three inputs) at the left end of the row, where the initial values of the six state pixels (which include the three truncated state pixels on the left) are -1 due to the boundary conditions, and the vector of three input pixels can take eight different values. The entire state/input block is then shifted right to pick up the next three input pixels, and the previous three input pixels become the middle three state pixels. The full-state trellis therefore has 64 states with 8 branches out of each state. The Chugg-style truncation scheme shown in Fig. 5 has eight states with eight branches out of each state; the deleted state pixels are estimated by surviving paths in the forward and backward passes of the MSM RS-SISO algorithm. At each position (m, n), the trellis branch output vector consists of three 3×3 inner products between the inverted mask and the pixel values defined by the trellis; the upper inner product feedback from two previously processed rows, the middle uses one feedback row, and the lower uses received pixels only. The branch metric is the squared Euclidean distance between the branch output and the received pixel vector $[r(m, n), r(m + 1, n), r(m + 2, n)]$.

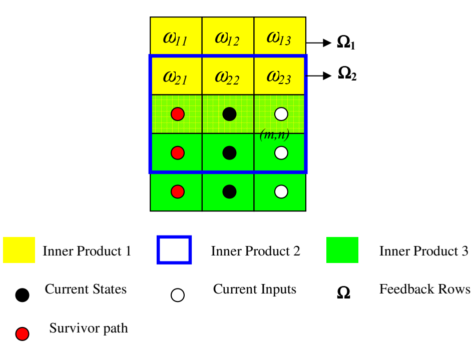

Fig. 5. 2D truncated state diagram for the forward row pass of the IRCSDF algorithm of [3] on a 3×3 ISI channel. MSM-RS-SISOs [8] are used in row and column directions.

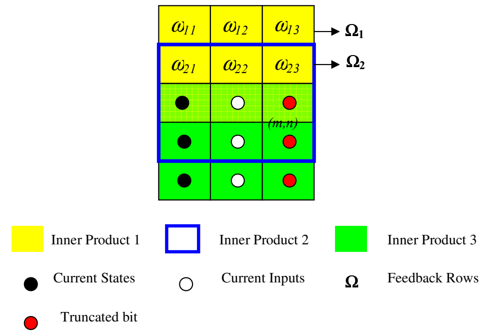

Fig. 6. New-style truncated state diagram for the forward row pass of the IRCSDF algorithm on a 3×3 ISI channel. The new MSM-RS-SISO algorithm of section 2 is used in row and column directions.

Fig. 6 shows the truncated state diagram for an IRCSDFA employing the new MSM-RS-SISO of section 2. This truncation scheme works well for center weighted masks in which the relative magnitude of the edge coefficients on each row (column) are much smaller than those of the center coefficient. As with the truncation scheme shown in Fig. 5, the truncated trellis has 8 states and 8 branches per state. Thus, both truncated IRCSDF algorithms are equivalent in complexity to an IRCSDFA which employs the M-BCJR algorithm with $M = 8$ in its row and column detectors; performance comparisons between these three algorithms are made in the following section.

3.1. Simulation Results

We consider the 3×3 channel mask with rows (top to bottom) $[0\ \alpha\ 0]$, $[\alpha\ 1\ \alpha]$, and $[0\ \alpha\ 0]$. We compare the performance of our proposed algorithm (corresponding to Fig. 6) with that of $M = 8$ M-BCJR [9] and Chugg's algorithm (corresponding to Fig. 5). The ML bound is also shown for comparison. The results for $\alpha = 0.1, 0.2$ are shown in Fig. 7; this figure also shows the results of simple hard decision demodulation for these channels. Fig. 8 depicts similar results for "Channel B" and the averaging mask. The 3×3 "Channel B" mask [10] has rows (top to bottom) $[c\ b\ c]$, $[b\ 1\ b]$, and $[c\ b\ c]$, where $b = 0.352$ and $c = 0.0993$; the 3×3 averaging mask has all elements equal to 1.0. Six iterations of the IRCSDF algorithm were used for all simulations shown in Fig. 7 and Fig. 8, with the exception of the hard-decision simulations.

When $\alpha = 0.1$, the performance of the new algorithm (0.7 dB away from ML bound) is better than that of the $M = 8$ M-BCJR algorithm (more than 6 dB away from ML bound). When $\alpha = 0.2$, the performance of the new algorithm (3 dB away from ML bound) is again better than that of $M = 8$ M-BCJR (5.5 dB away from

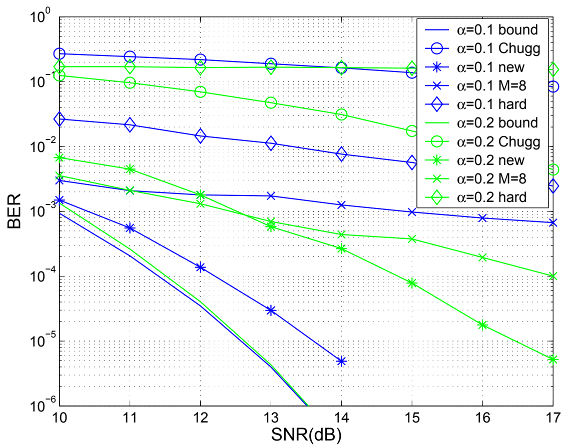

Fig. 7. 2D-ISI simulation results for two 3×3 center-weighted masks with 1 in the center tap, 0s in the corner taps, and 0.1 (respectively, 0.2) in the side taps.

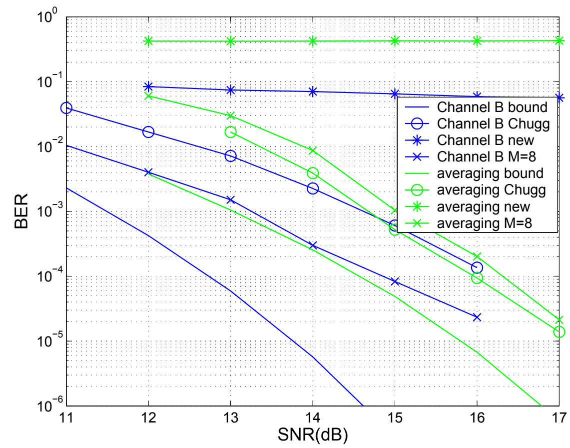

Fig. 8. 2D-ISI simulation results for two 3×3 masks. The "Channel B" mask has rows (top to bottom) $[c\ b\ c]$, $[b\ 1\ b]$, and $[c\ b\ c]$, where $b = 0.352$ and $c = 0.0993$. The averaging mask has all elements equal to 1.

ML bound). Chugg's algorithm fails for both $\alpha = 0.1, 0.2$, as does hard-decision demodulation. For Channel B, the performance of $M = 8$ M-BCJR (2 dB away from ML bound) is better than that of Chugg's algorithm (3.4 dB away from ML bound). For the averaging mask, the performance of Chugg's algorithm (1.3 dB away from ML bound) is better than that of $M = 8$ M-BCJR (1.8 dB away from ML bound). Our proposed algorithm fails for Channel B and the averaging mask. All comparisons are done at a BER of 10^{-4}.

4. CONCLUSIONS

This paper has developed and demonstrated a new reduced-state BCJR algorithm for detection on 1- and 2-dimensional finite-size ISI channels, that works especially well for center-weighted masks. This paper has also presented detailed performance comparisons between the newly proposed algorithm and two previously published algorithms, which point out the strengths and weaknesses of each algorithm. The 1D simulation results show that, for center-weighted masks, the proposed algorithm significantly outperforms the previously proposed MSM RS-SISO algorithm of [8]. However, the simulations also demonstrate that the M-BCJR algorithm of [9] gives by far the best performance for reduced-state 1D equalization, for both center-weighted and relatively "flat" ISI masks. The situation changes when the reduced-state algorithms are used in the row and column detectors of the 2D-ISI algorithm proposed in [3]. The newly proposed algorithm performs best for center weighted 2D masks with 0s in the corners, while the algorithm of [8] achieves the best performance for the averaging mask. The "Channel B" mask, based on sampling of a 2D Gaussian PDF [10], presented the most challenging test for all three algorithms; at high SNR, the best performing algorithm on "Channel B" was more than 2 dB away from the ML bound. We conclude that improved reduced-state algorithms are needed for 2D-ISI masks with Gaussian-like magnitude profiles.

5. REFERENCES

[1] L. R. Bahl, J. Cocke, F. Jelinek, and J. Raviv, "Optimal decoding of linear codes for minimizing symbol error rate," *IEEE Trans. Inform. Theory*, vol. 20, pp. 284–287, Mar. 1974.

[2] R. Koetter, A. C. Singer, and M. Tuechler, "Turbo equalization," *IEEE Signal Processing Magazine*, vol. 21, no. 1, pp. 67–80, Jan. 2004.

[3] T. Cheng, B. J. Belzer, and K. Sivakumar, "Row-column soft-decision feedback algorithm for two-dimensional intersymbol interference," *IEEE Sig. Proc. Letters*, vol. 14, pp. 433–436, July 2007.

[4] P. M. Njeim, T. Cheng, B. J. Belzer, and K. Sivakumar, "Image detection in 2D intersymbol interference with iterative soft-decision feedback zig-zag algorithm," in *Proc. 43rd annual Allerton Conf. on Comm., Computing, and Control*, Univ. of Illinois, Urbana-Champaign, IL, Sept. 2005, CD-ROM.

[5] M. Marrow and J. K. Wolf, "Iterative detection of 2-dimensional ISI channels," in *Proc. Info. Theory Workshop*, Paris, France, Mar./Apr. 2003, pp. 131–134.

[6] Y. Wu, J. A. O'Sullivan, N. Singla, and Ronald S. Indeck, "Iterative detection and decoding for separable two-dimensional intersymbol interference," *IEEE Trans. Magnetics*, vol. 39, no. 4, pp. 2115–2120, July 2003.

[7] G. Colavolpe, G. Ferrai, and R. Raheli, "Reduced-state BCJR-type algorithms," *IEEE Jour. on Sel. Areas in Commun.*, vol. 19, pp. 848–859, May 2001.

[8] X. Chen and K. M. Chugg, "Reduced-state soft-input/soft-output algorithms for complexity reduction in iterative and non-iterative data detection," in *Proc. 2000 IEEE International Conf. on Commun. (ICC 2000)*, New Orleans, LA, June 2000, vol. 1, pp. 6–10.

[9] C. Fragouli, N. Seshadri, and W. Turin, "Reduced-trellis equalization using the M-BCJR algorithm," *Wireless Commun. and Mobile Computing*, vol. 1, pp. 397–406, July 2001.

[10] Xiaopeng Chen and Keith M. Chugg, "Near-optimal data detection for two-dimensional ISI/AWGN channels using concatenated modeling and iterative algorithms," in *Proc. IEEE International Conference on Communications, ICC'98*, 1998, pp. 952–956.